Published in final edited form as:
Am J Ophthalmol. 2007 February ; 143(2): 272–279.

Scanning Laser Polarimetry with Variable and Enhanced Corneal Compensation in Normal and Glaucomatous Eyes

Mitra Sehi, PhD[1], **Delia C. Guaqueta, MD**[1], **William J. Feuer, MS**[1], and **David S. Greenfield, MD**[1] **Advanced Imaging in Glaucoma Study Group1,2,3,4,***

1 *Department of Ophthalmology, University of Miami Miller School of Medicine, Bascom Palmer Eye Institute, Palm Beach Gardens, FL*

2 *Cleveland Clinic Foundation, Cleveland, OH*

3 *University of Pittsburgh School of Medicine, Pittsburgh, PA*

4 *University of Southern California, Los Angeles, CA*

Abstract

Purpose—To investigate whether correction for atypical birefringence pattern (ABP) using scanning laser polarimetry with enhanced corneal compensation (SLP-ECC) reduces the severity of ABP compared with variable corneal compensation (SLP-VCC), and improves the correlation with visual function.

Design—Prospective observational study.

Methods—Normal and glaucomatous eyes enrolled from 4 clinical sites underwent complete examination, automated perimetry, SLP-ECC and SLP-VCC. Eyes were characterized in 3 groups based upon the typical scan score (TSS): normal birefringence pattern (NBP) was defined as TSS 80, mild ABP as TSS 61–79, moderate-severe ABP as TSS 60. For each of 4 SLP parameters the area under the ROC curve (AUROC) was calculated to compare the ability of SLP-ECC and SLP-VCC to discriminate between normal and glaucomatous eyes.

Results—Eighty-four normal volunteers and 45 glaucoma patients were enrolled. Mean TSS was significantly ($p<0.001$) greater using SLP-ECC (98.0 ± 6.6) compared to SLP-VCC (83.4 ± 22.5). The frequency of moderate-severe ABP images was significantly ($p<0.001$, McNemar test) higher using SLP-VCC (18 of 129, 14%) compared to SLP-ECC (1 of 129, 0.8%). Two SLP-ECC parameters (TSNIT average and inferior average) had significantly ($p=0.01$, $p<0.001$) higher correlation ($r=0.45$, $r=0.50$ respectively) with MD compared to SLP-VCC ($r=0.34$, $r=0.37$). Among eyes with moderate-severe ABP (N = 18), inferior average obtained using SLP-ECC had significantly ($p=0.03$) greater AUROC (0.91 ± 0.07) compared with SLP-VCC (0.78 ± 0.11).

Inquiries to: David Greenfield, MD, Bascom Palmer Eye Institute, University of Miami Miller School of Medicine, 7101 Fairway Drive, Palm Beach Gardens, FL 33418, USA. Phone: (561) 515-1500; Fax: (561) 355-8616; Email: dgreenfield@med.miami.edu.
*See www.AIGStudy.net for the full list of authors.

This study was supported in part by NIH Grants R01-EY013516, R01-EY08684, Bethesda, Maryland; the Maltz Family Endowment for Glaucoma Research, Cleveland, Ohio; a grant from Mr. Barney Donnelley, Palm Beach, FL; The Kessel Foundation, Bergenfield, New Jersey; and an unrestricted grant from Research to Prevent Blindness, New York, New York.

The authors have no financial interest in any device or technique described in this paper. Dr. Greenfield has received research support and has served as a consultant for Carl Zeiss Meditec.

Conclusions—SLP-ECC significantly reduces the frequency and severity of ABP compared to SLP-VCC and improves the correlation between RNFL measures and visual function.

Introduction

The basic pathologic change in glaucoma is loss of retinal ganglion cells and their axons resulting in retinal nerve fiber layer (RNFL) atrophy and the optic nerve head changes characteristic of glaucoma. Scanning laser polarimetry (SLP) is a confocal scanning laser ophthalmoscope with an integrated polarimeter that measures the amount of retardation (phase shift) of a polarized near-infrared laser beam as it passes through the RNFL.[1-6] In order to neutralize the confounding influence of corneal birefringence on RNFL thickness, the latest commercial polarimeter has an integrated variable corneal compensator, which determines and neutralizes eye-specific corneal polarization axis and magnitude using the concept of the macula as an intraocular polarimeter.[6–8] Several studies have shown that SLP with variable corneal compensation (VCC) significantly improves the structure-function relationship,[9-16] the agreement with other imaging technologies,[10, 17–19] and the discriminating power for glaucoma detection[2, 8, 20, 21] as compared to scanning laser polarimetry with fixed corneal compensation. Macular pathology, however, may introduce error in the strategy used for corneal compensation and alternative strategies have been proposed.[6, 17]

Despite adequate corneal compensation (images with residual corneal birefringence of 13 nm based upon personal communication, Q Zhou, Ph.D., Carl Zeiss Meditec, Dublin, CA), some SLP-VCC scans are characterized by atypical birefringence patterns (ABP) such that the brightest areas of the retardation maps are not consistent with the histologically thickest portions of the peripapillary RNFL located along the superior and inferior arcuate bundles. Eyes with ABP are characterized by variable areas of high retardation arranged in a spoke-like peripapillary pattern, often with areas of high retardation nasally and temporally.[22] Proposed mechanisms for atypical images include older age, myopia and thinner retinal pigment epithelium. A support vector machine score (typical scan score, TSS) ranging from 0 – 100 has been reported to be highly predictive of ABP; lower scores are highly correlated with atypical patterns and may confound the detection of glaucoma.[22, 23]

An enhancement module (enhanced corneal compensation, ECC) has been recently described to improve the signal-to-noise ratio and eliminate artifacts associated with ABP.[23, 24] The ECC algorithm introduces a predetermined birefringence bias to shift the measurement of the total retardation to a higher value region to remove noise and reduce atypical patterns.[23] The amount of birefringence bias is determined using the birefringence pattern of the macular region, and then is mathematically removed point by point from the total birefringence pattern of the VCC to improve the signal and obtain a retardation pattern of the RNFL with least noise.[23] The purpose of this study was to examine the hypothesis that correction for ABP using SLP with ECC reduces the frequency and severity of ABP compared with VCC, and improves the correlation between SLP parameters and visual function.

Patients and Methods

* Refer to www.AIGStudy.net for the full manual of procedures for the AIG Study *

Normal and glaucomatous eyes meeting eligibility criteria were enrolled in this prospective study from four clinical sites: Bascom Palmer Eye Institute (Palm Beach Gardens, FL), University of Pittsburgh Medical Center (Pittsburgh, PA), University of Southern California (Los Angeles, CA), and Cleveland Clinic Foundation (Cleveland, OH). Informed consent was obtained from all subjects by means of a consent form approved by the Institutional Review Boards for Human Research at each site. All patients underwent complete ophthalmic

examination including slit lamp biomicroscopy, gonioscopy, Goldmann applanation tonometry, ultrasound pachymetry, dilated stereoscopic examination and photography of the optic disc, standard automated perimetry (SAP) using the Humphrey Field Analyzer (Carl-Zeiss Meditec, Dublin, CA) SITA Standard strategy program 24-2, and SLP imaging (Carl-Zeiss Meditec, Dublin, CA) using variable (VCC) and enhanced corneal compensation (ECC).

Inclusion criteria common to both groups consisted of best corrected visual acuity equal to or better than 20/40, refractive error between -7.00D and +3.00D, age range between 40 and 79 years, reliable SAP (less-than-33% rate of fixation losses, false positives and false negatives), and no prior intraocular surgery except for uncomplicated cataract extraction. Eyes with ocular disease other than glaucoma or cataract, visual acuity less than 20/40, peripapillary atrophy extending to 1.7 mm from disc center, retinal disease, or unreliable SAP were excluded. Normal subjects consisted of volunteers such as office employees, and friends or family members of glaucoma patients. Normal subjects had no history of ocular disease except cataract, intraocular pressure (IOP) less than or equal to 21 mmHg by Goldmann applanation tonometry, normal optic disc appearance based upon clinical stereoscopic examination and review of stereodisc photography. All eyes had two normal SAP examinations defined as glaucoma hemifield test within normal limits, and mean and pattern standard deviation of probability > 5%. Absence of glaucomatous optic neuropathy was defined as vertical cup-disc asymmetry less than 0.2, and intact neuroretinal rim without peripapillary hemorrhages, notches, localized pallor, or RNFL defect. Glaucomatous optic neuropathy was defined as either cup/disc asymmetry between fellow eyes of greater than 0.2, rim thinning, notching, excavation, or RNFL defect. Glaucoma patients had glaucomatous optic nerve damage and corresponding abnormal SAP defined as abnormal glaucoma hemifield test and pattern standard deviation outside 95% normal limits. Patients with SAP abnormalities had at least one confirmatory visual field examination. If both eyes satisfied inclusion criteria, one eye was randomly selected for enrolment.

SLP imaging (software version 5.5.0) was performed in a standardized fashion at all sites through undilated pupils. Three consecutive scans were obtained using VCC and ECC on the same day by the same examiner. A primary scan was obtained prior to each measurement to compensate for the corneal birefringence. Images that were obtained during eye movement were excluded, as well as unfocused, poorly centered images, or images with a quality score grade < 8. One eye of each volunteer was randomly selected for the analysis. A fixed concentric measurement band centered on the optic disc with a 3.2mm outer and a 2.4mm inner diameter was used to generate the peripapillary retardation measurements. SLP parameters used as outcome measures for this investigation included: TSNIT (temporal superior nasal inferior temporal) average, superior average, inferior average, TSNIT-SD (temporal superior nasal inferior temporal-standard deviation) and the typical scan score (TSS).

Eyes were stratified in three groups based upon the birefringence pattern and TSS score. The determination of birefringence pattern group was made based on the TSS score of VCC measurements. Normal birefringence pattern (NBP) was defined as a TSS value of 80 or greater, mild ABP was defined as a TSS value of 61 – 79, and severe ABP was defined as a TSS value of 60 or lower. This was based upon a prior study[22] that demonstrated a strong correlation between ABP severity and TSS score and 100% probability of ABP in retardation images with TSS scores of 60 or less using multiple logistic regression analysis. Statistical analysis was performed using SPSS version 13.0 (SPSS Inc., Chicago, IL). Pearson correlation coefficients were calculated and compared using a test of homogeneity with correlated data, [25] and Chi-square test and independent samples T-test were used to compare different measures between groups. For each of four SLP parameters the area under the ROC curve (AUROC) was calculated to compare the ability of ECC and VCC to discriminate between normal and glaucomatous eyes. Linear regression was used to estimate the effect of age on

SLP parameters in the control group and these relationships were used to adjust measurements in both groups to the same age prior to calculation of AUROCs. Significant differences in AUROC were determined using the method of Hanley and McNeil.[26] A p value of less than or equal to 0.05 was considered statistically significant.

Results

One hundred and twenty nine eyes of 129 patients (84 normal, 45 glaucoma) were enrolled (mean age 52.9 ± 9.8, 62.4 ± 8.7 years, respectively). The clinical characteristics of the study population are summarized in Table 1. The central corneal thickness was significantly (p=0.03) less in the glaucoma group (544.2 ± 38.0 microns) compared to the normal group (559.7 ± 36.6 microns). The average visual field mean deviation and pattern standard deviation was significantly (p<0.001) worse in the glaucoma group compared to the normal group.

Figure 1 illustrates a glaucomatous right eye with ABP. The top images demonstrate glaucomatous cupping (left) and corresponding visual field defect (pattern deviation plot) using standard automated perimetry (right). The bottom left image illustrates the SLP-VCC scan with ABP characterized by spoke-like areas of high retardation (TSS = 17) particularly evident in the nasal and temporal regions. The bottom right image illustrates the SLP-ECC scan demonstrating superior RNFL loss (TSS = 94).

Table 2 summarizes the SLP parameters obtained using ECC and VCC. The frequency of mild and moderate-severe ABP was significantly (p<0.001, McNemar test) higher using VCC (12.3% and 13.8%, respectively) compared to ECC (0% and 0.8%, respectively). ECC provided significantly (p<0.001) lower TSNIT average values and significantly (p<0.001) greater TSNIT-SD values compared with VCC.

Table 3 illustrates the AUROC ± SE for each of 4 SLP parameters obtained with ECC and VCC. As our normal group was significantly younger than the glaucoma group, the AUROC were adjusted for age. ECC and VCC had similar performance in eyes with NBP and mild ABP. In eyes with moderate-severe ABP, inferior average RNFL thickness obtained using ECC (Figure 2) had the highest AUROC (0.91±0.07) and was significantly (p=0.03) greater compared to VCC (0.75 ± 0.12).

Table 4 demonstrates the association between SLP parameters obtained with ECC and VCC and visual field MD and PSD. Two ECC parameters (TSNIT average and inferior average) had significantly (p=0.01, p<0.001 respectively) higher correlation (r=0.45, r=0.50 respectively) with visual field MD compared to their equivalent VCC parameters (r=0.34, r=0.37). One ECC parameter (inferior average) had significantly (p=0.01) higher correlation (r= −0.55) with visual field PSD compared to its equivalent VCC parameter (r= −0.46).

We calculated the correlation between the TSS value as a measure of atypia, and visual field MD and PSD as measures of glaucomatous damage, to evaluate the relationship between glaucomatous visual field loss and severity of ABP. We found no significant correlation between TSS and MD (r = 0.09, p = 0.28), or TSS and PSD (r = 0.003, p = 0.97) across the entire cohort. Among the subgroup of eyes with glaucoma, we similarly found no correlation between TSS and MD (r = 0.04, p = 0.81), and TSS and PSD (r = 0.14, p = 0.36).

Discussion

SLP is a useful imaging technology for glaucoma diagnosis and monitoring. Currently in its fifth commercial iteration, considerable progress has been made in reducing artifact originating from uncompensated anterior segment birefringence.[1, 6–8, 27] ABP images represent a challenge to SLP image interpretation by unfavourably altering the signal-to-noise ratio. ABP

images have been reported to be more prevalent in older and myopic patients.[22] The mechanism remains obscure and is thought to be associated with reduced retinal pigment epithelial pigmentation and/or anomalous reflections from the posterior segment back to the detector.

ECC represents a novel strategy for correction of ABP images by introducing a birefringence bias determined using the birefringence pattern of the macular region, which is then mathematically removed point by point from the total birefringence pattern of the VCC image to improve the signal and obtain a retardation pattern of the RNFL with reduced noise.[23] Toth et al[23] reported a 10 – 15% prevalence of ABP images among a population of 27 glaucoma patients and 19 normal subjects and found that the ECC algorithm improved the mean TSS values. Sehi et al[28] reported that ECC parameters maintained a high level of repeatability as compared with VCC. Our data demonstrates that ECC reduces ABP images in normal and glaucomatous eyes as judged by TSS values. Earlier work by Bagga et al[22] found the predictive probability of ABP in eyes with TSS values above 60 was 100%. Thus, using a TSS cut-off value of 60 for defining moderate to severe atypia, our data demonstrates a significant reduction in the frequency of ABP (14% using VCC, 1% using ECC). Furthermore, the severity of ABP was reduced using the ECC algorithm. Mean TSS values were significantly greater using ECC (mean TSS = 98) compared to VCC (mean TSS = 83). Further study is necessary to explain why ECC failed to correct significant image atypia (TSS value of 38) in one glaucomatous eye among our series.

Several studies have examined the association between SLP structural measures and visual function. [9–14, 29, 30] As compared to fixed corneal compensation, data has shown that SLP using VCC provides increased correlation with visual function,[2] greater discriminating power for glaucoma detection,[8] and greater correlation with RNFL assessments obtained with optical coherence tomography (OCT).[10] In the present study, the ECC module significantly improved the association between several RNFL parameters and visual field mean deviation and pattern standard deviation. One should recognize that structure and function may not always be well correlated in glaucoma[31–34] and often there is disagreement even among various optical imaging instruments when assessing structural damage[35].

For each of 4 SLP parameters, we compared the ability of ECC and VCC to discriminate between normal and glaucomatous. Overall, the best performing parameter using ECC was the inferior average RNFL thickness. In contrast, others [15, 36–38] have reported the nerve fiber indicator (NFI) to be the most robust SLP parameter for glaucoma detection. Calculation of a similar parameter for ECC using either a neural network strategy or machine learning classifier [37] may provide additional information to assist the clinician in glaucoma diagnosis.

We found that the diagnostic performance of ECC was significantly improved only in eyes with moderate-severe ABP, which we define as a TSS value of 60 or less. It would therefore be of apparent benefit to utilize this algorithm in images with unfavourable signal-to-noise ratio. Similarly, one may speculate that eyes with a reduced retardance signal due to advanced glaucomatous RNFL atrophy may benefit from ECC imaging. Such eyes are characterized by low retardance values and by superimposing the RNFL birefringence onto a large predetermined birefringence one shifts the retardation measurement into a more sensitive region of the signal amplitude/retardance curve.[39] While all four of the SLP parameters had higher AUROC with ECC than VCC, our study found a significant difference only in the group of eighteen subjects most severely affected with abnormal birefringence pattern, and only in the inferior thickness parameter.

It is important to point out that there are limitations to using the AUROC to assess glaucoma diagnostic tests[40], and recent data suggests that covariates such as optic disc size[12] should be

taken into account when comparing the diagnostic performance of such tests. This would not likely be a confounding factor in our study as the impact of disc size upon RNFL assessment would be similar using both VCC and ECC. While ECC inferior average performed significantly better than VCC inferior average for discriminating between our normal and glaucoma patients with moderate to severe ABP, the efficacy of discrimination may be different in subjects with different ages or in other clinically important subgroups, such as different races. In our study, we have not adjusted the p-values for multiple comparisons as these parameters are not independent and highly correlated, thus the true alpha error associated with inferior average could be higher than 0.03. Finally, the AUROCs may be inflated to the extent that patients referred to a glaucoma practice who do not have glaucoma, could have SLP responses different from the normal controls used in this study.

In conclusion, SLP using ECC significantly reduces the frequency and severity of ABP compared to SLP using VCC and improves the correlation between RNFL thickness measures and visual function. In eyes with moderate-severe ABP, the ECC algorithm may improve the discriminating power of SLP.

References

1. Greenfield DS, Huang X-R, Knighton RW. Effect of corneal polarization axis on assessment of retinal nerve fiber layer thickness by scanning laser polarimetry. Am J Ophthalmol 2000;129:715–22. [PubMed: 10926978]
2. Choplin NT, Zhou Q, Knighton RW. Effect of individualized compensation for anterior segment birefringence on retinal nerve fiber layer assessments as determined by scanning laser polarimetry. Ophthalmology 2003;110:719–25. [PubMed: 12689893]
3. Huang XR, Knighton RW. Microtubules contribute to the birefringence of the retinal nerve fiber layer. Invest Ophthalmol Vis Sci 2005;46:4588–93. [PubMed: 16303953]
4. Huang XR, Knighton RW. Theoretical model of the polarization properties of the retinal nerve fiber layer in reflection. Appl Opt 2003;42:5726–36. [PubMed: 14528936]
5. Huang XR, Knighton RW. Diattenuation and polarization preservation of retinal nerve fiber layer reflectance. Appl Opt 2003;42:5737–43. [PubMed: 14528937]
6. Knighton RW, Huang X-R, Greenfield DS. Analytical model of scanning laser polarimetry for retinal nerve fiber layer assessment. Invest Ophthalmol Vis Sci 2002;43:383–92. [PubMed: 11818381]
7. Garway-Heath DF, Greaney MJ, Caprioli J. Correction for the erroneous compensation of anterior segment birefringence with the scanning laser polarimeter for glaucoma diagnosis. Invest Ophthalmol Vis Sci 2002;43:1465–74. [PubMed: 11980862]
8. Weinreb RN, Bowd C, Zangwill LM. Glaucoma detection using scanning laser polarimetry with variable corneal polarization compensation. Arch Ophthalmol 2003;121:218–24. [PubMed: 12583788]
9. Schlottman PG, De Cilla S, Greenfield DS, Caprioli J, Garway-Heath DF. Relationship between visual field sensitivity and retinal nerve fiber layer thickness as measured by scanning laser polarimetry. Invest Ophthalmol Vis Sci 2004;45:1823–9. [PubMed: 15161846]
10. Bagga H, Greenfield DS, Feuer W, Knighton RW. Scanning laser polarimetry with variable corneal compensation and optical coherence tomography in normal and glaucomatous eyes. Am J Ophthalmol 2003;135:521–9. [PubMed: 12654370]
11. Bowd C, Zangwill LM, Weinreb RN. Association between scanning laser polarimetry measurements using variable corneal polarization compensation and visual field sensitivity in glaucomatous eyes. Arch Ophthalmol 2003;121:961–6. [PubMed: 12860798]
12. Medeiros FA, Zangwill LM, Bowd C, Sample PA, Weinreb RN. Influence of disease severity and optic disc size on the diagnostic performance of imaging instruments in glaucoma. Invest Ophthalmol Vis Sci 2006;47:1008–15. [PubMed: 16505035]
13. Mohammadi K, Bowd C, Weinreb RN, Medeiros FA, Sample PA, Zangwill LM. Retinal nerve fiber layer thickness measurements with scanning laser polarimetry predict glaucomatous visual field loss. Am J Ophthalmol 2004;138:592–601. [PubMed: 15488786]

14. Hoffmann EM, Medeiros FA, Sample PA, et al. Relationship between patterns of visual field loss and retinal nerve fiber layer thickness measurements. Am J Ophthalmol 2006;141:463–471. [PubMed: 16490491]
15. Reus NJ, Lemij HG. Scanning laser polarimetry of the retinal nerve fiber layer in perimetrically unaffected eyes of glaucoma patients. Ophthalmology 2004;111:2199–203. [PubMed: 15582074]
16. Da Pozzo S, Fuser M, Vattovani O, Di Stefano G, Ravalico G. GDx-VCC performance in discriminating normal from glaucomatous eyes with early visual field loss. Graefes Arch Clin Exp Ophthalmol 2006;244:689–695. [PubMed: 16292656]
17. Bagga H, Greenfield DS, Knighton RW. Scanning laser polarimetry with variable corneal compensation: Identification and correction for corneal birefringence in eyes with macular pathology. Invest Ophthalmol Vis Sci 2003;44:1969–76. [PubMed: 12714631]
18. Greenfield DS, Bagga H, Knighton RW. Macular thickness changes in glaucomatous optic neuropathy detected using optical coherence tomography. Arch Ophthalmol 2003;121:41–6. [PubMed: 12523883]
19. Essock EA, Sinai MJ, Bowd C, Zangwill LM, Weinreb RN. Fourier analysis of optical coherence tomography and scanningn laser polarimetry retinal nerve fiber layer measurements in the diagnosis of glaucoma. Arch Ophthalmol 2003;121:1238–45. [PubMed: 12963606]
20. Greenfield DS, Knighton RW, Feuer W, Schiffman J, Zangwill L, Weinreb RN. Correction for corneal polarization axis improves the discriminating power of scanning laser polarimetry. Am J Ophthalmol 2002;134:27–33. [PubMed: 12095804]
21. Tannenbaum D, Hoffman D, Lemij HG, Garway-Heath DF, Greenfield DS, Caprioli J. Variable corneal compensation improves the discrimination between normal and glaucomatous eyes with the scanning laser polarimeter. Ophthalmology 2004;111:259–64. [PubMed: 15019373]
22. Bagga H, Greenfield DS, Feuer W. Quantitative assessment of atypical birefringence images using scanning laser polarimetry with variable corneal compensation. Am J Ophthalmol 2005;139:437–46. [PubMed: 15767051]
23. Toth M, Hollo G. Enhanced corneal compensation for scanning laser polarimetry on eyes with atypical polarisation pattern. Br J Ophthalmol 2005;89:1139–42. [PubMed: 16113368]
24. Da Pozzo S, Marchesan R, Canziani T, Vattovani O, Ravalico G. Atypical pattern of retardation on GDx-VCC and its effect on retinal nerve fibre layer evaluation in glaucomatous eyes. Eye 2006;20:769–75. [PubMed: 16021190]
25. Meng XL, Rosenthal R, Rubin DB. Comparing correlated correlation coefficients. Psych Bull 1992;111:172–5.
26. Hanley JA, McNeil BJ. A method of compring the areas under receiver operating curves derived from the same cases. Radiology 1983;148:839–43. [PubMed: 6878708]
27. Zhou Q, Weinreb RN. Individualized compensation of anterior segment birefringence during scanning laser polarimetry. Invest Ophthalmol Vis Sci 2002;43:2221–8. [PubMed: 12091420]
28. Sehi M, Guaqueta DC, Greenfield DS. An enhancement module to improve the atypical birefringence pattern using scanning laser polarimetry with variable corneal compensation. Br J Ophthalmol 2006;90:749–53. [PubMed: 16481378]
29. Gunvant P, Zheng Y, Essock EA, et al. Predicting subsequent visual field loss in glaucomatous subjects with disc hemorrhage using retinal nerve fiber layer polarimetry. J Glaucoma 2005;14:20–5. [PubMed: 15650599]
30. Reus NJ, Lemij HG. The relationship between standard automated perimetry and GDxVcCC measurements. Invest Ophthalmol Vis Sci 2004;45:840–5. [PubMed: 14985299]
31. Bagga H, Feuer WJ, Greenfield DS. Detection of psychophysical and structural injury in eyes with glaucomatous optic neuropathy and normal standard automated perimetry. Arch Ophthalmol 2006;124:169–76. [PubMed: 16476885]
32. Bagga H, Greenfield DS. Quantitative assessment of structural damage in eyes with localized visual field abnormalities. Am J Ophthalmol 2004;137:797–805. [PubMed: 15126142]
33. Johnson CA, Sample PA, Cioffi GA, Liebmann JM, Weinreb RN. Structure and function evaluation (SAFE) I. Criteria for glaucomatous visual field loss using standard automated perimetry (SAP) and short wavelength automated perimetry (SWAP). Am J Ophthalmol 2002;134:177–85. [PubMed: 12140023]

34. Johnson CA, Sample PA, Zangwill LM, et al. Structure and function evaluation (SAFE) II. Comparison of optic disk and visual field characteristics. Am J Ophthalmol 2003;135:148–54. [PubMed: 12566017]

35. Hoffmann EM, Bowd C, Medeiros FA, et al. Agreement among 3 Optical Imaging Methods for the Assessment of Optic Disc Topography. Ophthalmology 2005;112:2149–56. [PubMed: 16219355]

36. Medeiros FA, Zangwill LM, Bowd C, Weinreb RN. Comparison of the GDxVCC scanning laser polarimeter, HRT II confocal scanning laser ophthalmoscope, and Stratus OCT optical coherence tomograph for the detection of glaucoma. Arch Ophthalmol 2004;122:827–37. [PubMed: 15197057]

37. Bowd C, Medeiros FA, Zhang Z, et al. Relevance vector machine and support vector machine classifier analysis of scanning laser polarimetry retinal nerve fiber layer measurements. Invest Ophthalmol Vis Sci 2005;46:1322–9. [PubMed: 15790898]

38. Medeiros FA, Zangwill LM, Bowd C, Mohammadi K, Weinreb RN. Comparison of scanning laser polarimetry using variable corneal compensation and retinal nerve fiber layer photography for detection of glaucoma. Arch Ophthalmol 2004;122:698–704. [PubMed: 15136317]

39. Knighton, RW.; Zhou, Q. New techniques. In: Iester, M.; Garway-Heath, DF.; Lemij, HG., editors. Optic nerve head and retinal nerve fibre analysis. Savona, Italy: Dogma; 2005. p. 117-119.

40. Medeiros FA, Sample PA, Zangwill LM, Liebmann JM, Girkin CA, Weinreb RN. A statistical approach to the evaluation of covariate effects on the receiver operating characteristic curves of diagnostic tests in glaucoma. Invest Ophthalmol Vis Sci 2006;47:2520–7. [PubMed: 16723465]

Appendix

AIGS STUDY GROUP

David S. Greenfield MD*, Carolyn D. Quinn MD, Mitra Sehi PhD. University of Miami Miller School of Medicine, Bascom Palmer Eye Institute, Palm Beach Gardens, FL.

Rohit Varma MD MPH*, Vikas Chopra MD, Brian Francis MD, David Huang MD PhD, Don Minckler MD, Ou Tan PhD. University of Southern California Keck School of Medicine, Doheny Eye Institute, Los Angeles, CA.

Scott D. Smith MD MPH*, Edward J. Rockwood MD. Cleveland Clinic Foundation, Cole Eye Institute, Cleveland, OH.

Joel S. Schuman MD*, Robert Noecker MD, Zvia Eliash MD, Hiroshi Ishikawa MD, Gadi Wollstein MD, Larry Kagemann MS. University of Pittsburgh Medical Center, University of Pittsburgh School of Medicine, Pittsburgh, PA.

*Principal Investigator

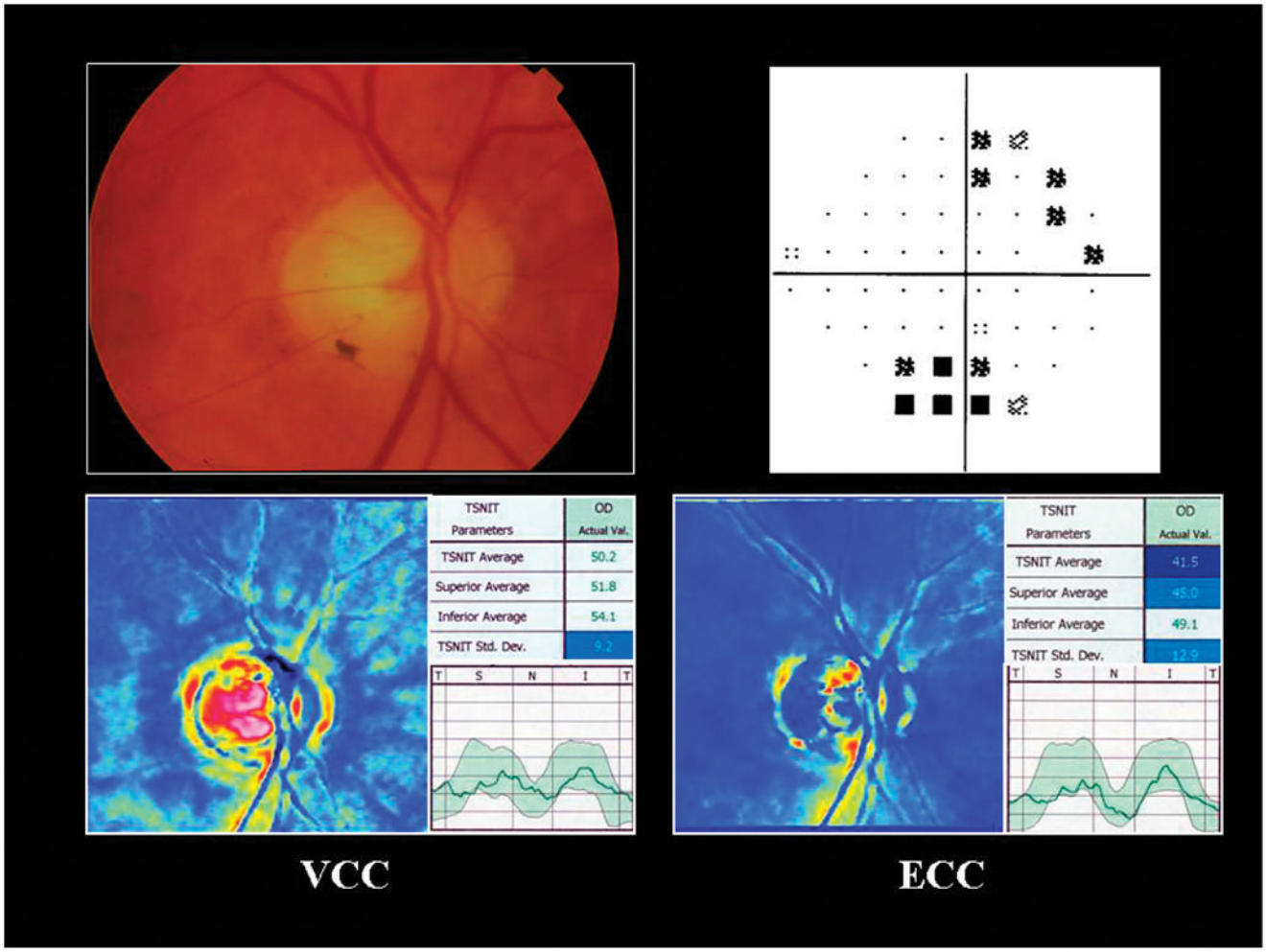

Figure 1.

Atypical birefringence pattern. Optic nerve photograph of a glaucomatous right eye (top left) and corresponding visual field defect using standard automated perimetry (top right). The bottom left image illustrates the variable corneal compensation scan with atypical birefringence pattern characterized by spoke-like areas of high retardation (typical scan score = 17) particularly evident in the nasal and temporal regions. The bottom right image illustrates the enhanced corneal compensation scan demonstrating superior retinal nerve fiber layer atrophy (typical scan score = 94).

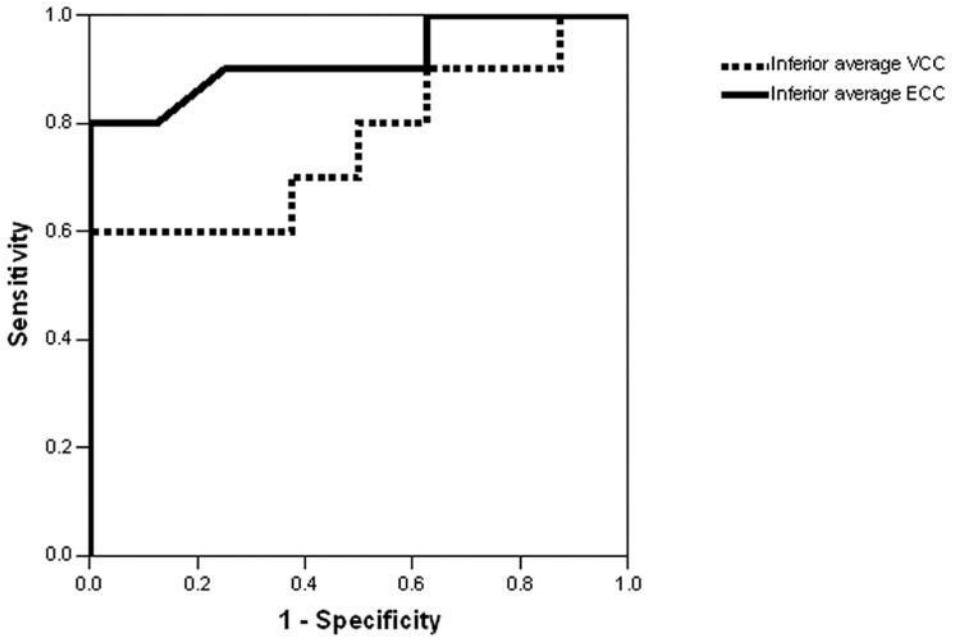

Figure 2.

Discriminating power of inferior average thickness using enhanced corneal compensation compared with variable corneal compensation in normal and glaucomatous eyes. Receiver operator characteristic (ROC) curve for inferior average thickness illustrates a significantly (p=0.03) increased area under the ROC curve using enhanced corneal compensation (0.92 ±0.07, solid line) as compared to VCC (0.76 ± 0.12, dotted line) in eyes with moderate to severe atypical birefringence pattern.

Table 1

Demographic, visual field, and scanning laser polarimetry characteristics of the study population (n=129) consisting of normal and glaucomatous eyes.

	Normal (n=84)	Glaucoma (n=45)	p-value
Age (years)	52.9 ± 9.8 (40–78)	62.4 ± 8.7 (40–77)	<0.001*
Gender			0.08‡
Male	22	19	
Female	62	26	
Race			0.09‡
White Non-Hispanic	59 (70%)	32 (71%)	
Black	9 (11%)	4 (9%)	
Asian	1 (1%)	4 (9%)	
Pacific Islander/Hawaiian	0 (0%)	1 (2%)	
Hispanic	15 (18%)	4 (9%)	
Central corneal thickness (μm)	559.7 ± 36.6 (500–658)	544.2 ± 38.0 (461–677)	0.03*
Visual field mean deviation (dB)	−0.3 ± 1.5	−4.3 ± 4.5	<0.001*
	(−5.5 to 2.9)	(−16.6 to 4.3)	
Visual field pattern standard deviation (dB)	1.6 ± 0.3 (1.0–2.7)	5.4 ± 4.2 (1.2–15.1)	<0.001*
SLP birefringence pattern			0.14‡
Normal birefringence pattern	65	30	
Mild abnormal birefringence pattern	11	5	
Moderate-severe abnormal birefringence pattern	8	10	

‡Chi-square test;

*Independent samples T-test; SLP = scanning laser polarimetry

Table 2

Scanning laser polarimetry parameters using variable (VCC) and enhanced (ECC) corneal compensation in normal and glaucomatous eyes.

SLP parameters	Normal (n=84)			Glaucoma (n=45)		
Mean ± SD (range)	VCC	ECC	p-value	VCC	ECC	p-value
TSNIT average	58.5 ± 5.9 (48.0–74.0)	55.5 ± 5.1 (46–55.5)	<0.001	48.5 ± 8.6 (33–79)	44.8 ± 6.8 (31.3–58.0)	<0.001
Superior average	70.0 ± 8.3 (43.6–89.0)	69.4 ± 7.5 (53.6–69.3)	0.13	56.9 ± 9.6 (33–75.3)	55.9 ± 9.8 (32.0–77.0)	0.16
Inferior average	68.2 ± 8.3 (50–94.3)	69.0 ± 8.0 (51.0–87.0)	0.27	54.0 ± 13.2 (23.7–93.0)	53.0 ± 10.8 (24.0–73.0)	0.15
TSNIT SD	24.0 ± 4.4 (14.0–33.0)	28.6 ± 3.9 (22–45)	<0.001	17.3 ± 4.7 (10–30)	21.4 ± 4.9 (12.9–32.0)	<0.001
Typical Scan Score	85.7 ± 19.9(4–100)	98.0 ± 4.7(70–100)	<0.001	79.2 ± 26.5(0–100)	98.0 ± 9.3(38–100)	<0.001

SLP = scanning laser polarimetry; VCC = variable corneal compensation; ECC = enhanced corneal compensation; SD = standard deviation; TSNIT = temporal superior nasal inferior temporal

Table 3

Age-adjusted areas under receiver operator characteristic curves (AUROC) discriminating between normal and glaucoma patients with normal birefringence pattern (NBP), mild abnormal birefringence pattern (ABP), and moderate-severe ABP.

SLP parameters	NBP (n=95)			Mild ABP (n=16)			Moderate-severe ABP (n=18)		
	VCC	ECC	p-value	VCC	ECC	p-value	VCC	ECC	p-value
TSNIT average	0.91 ±0.04	0.90 ±0.04	0.94	0.96 ±0.05	0.91 ±0.08	0.36	0.78 ±0.12	0.85 ±0.09	0.29
Superior average	0.85 ±0.05	0.86 ±0.05	0.74	0.84 ±0.10	0.78 ±0.12	0.15	0.70 ±0.14	0.80 ±0.11	0.31
Inferior average	0.86 ±0.05	0.88 ±0.04	0.48	0.89 ±0.09	0.86 ±0.10	0.65	0.75 ±0.12	0.91 ±0.07	0.03
TSNIT SD	0.82 ±0.05	0.85 ±0.05	0.46	0.82 ±0.11	0.73 ±0.15	0.50	0.78 ±0.11	0.88 ±0.08	0.28

ABP = atypical birefringence pattern; NBP = normal birefringence pattern; SE = standard error; VCC = variable corneal compensation; ECC = enhanced corneal compensation; TSNIT = temporal superior nasal inferior temporal

Table 4

Association between scanning laser polarimetry parameters obtained using enhanced (ECC) and variable (VCC) corneal compensation and visual field mean deviation (MD) and pattern standard deviation (PSD) among normal and glaucomatous eyes (n = 129).

	MD			PSD		
SLP parameters	**VCC[≠]**	**ECC[≠]**	**p-value[*]**	**VCC[≠]**	**ECC[≠]**	**p-value[*]**
TSNIT average	0.34	0.45	0.01	−0.48	−0.54	0.13
Superior average	0.39	0.41	0.56	−0.46	−0.47	0.76
Inferior average	0.37	0.50	<0.001	−0.46	−0.55	0.01
TSNIT SD	0.37	0.43	0.28	−0.40	−0.44	0.47

MD = mean deviation; PSD = pattern standard deviation; SLP = scanning laser polarimetry; VCC = variable corneal compensation; ECC = enhanced corneal compensation; TSNIT = temporal superior nasal inferior temporal.

[*] Test of homogeneity,

[≠] Pearson correlation coefficient